International Journal of Recent Technology and Engineering (IJRTE)
ISSN: 2277-3878 (Online), Volume-8 Issue-4, November 2019

Geomagnetic Induced Current Measurement in Hybrid PV-Wind System Transformers

Z M Khurshid, N F Ab Aziz, M Z A Ab Kadir, Z A Rhazali

Abstract: ***Geo magnetically induced currents (GICs) can cause saturation of the magnetic core of transformers in a power system. This saturation can conduce to generating harmonic currents, voltage-control problems and overheating of the transformer internal components, leading to gas relay alarm/operation and possible damage. In this work, GICs effects have been analyzed on hybrid PV-wind system transformers. The system implemented through using Power System Computer Aided Design (PSCAD/EMTDC) platform and made up of 2.1 MW wind farm, 2 MW solar photovoltaic (PV) farm, power storage system and load. Then the system is integrated with 33 kV grids through a 480V AC bus and step-up wye/delta transformer. In addition, Pi-section has been used between different parts of the system. The GIC is modeled as a controlled DC voltage source and inserted into the system through a neutral point of a wind turbine (WT) transformer. The simulation results of reactive power, voltage and current waveforms, and non-linear behavior due to asymmetric saturation of the magnetic core in the transformer due to 100 A GIC current injections are obtained. Moreover, different GIC blocking devices have been applied to mitigate or eliminate the flow of GIC to the system.***

Keywords: Geo magnetically induced currents, Hybrid, PV and Wind Turbine

I. INTRODUCTION

One of the most hazardous phenomena associated with space weather and solar activities is geomagnetic-induced currents (GIC) which is induced by the geoelectric field on the surface of the Earth during geomagnetic disturbance (GMD). This is a very low-frequency quasi-dc current (less than 1 Hz) with typical amplitudes of 10–15 A and up to 100 A peak current for 1–2 min that flows along conductors and modern technological infrastructures such as gas and oil pipelines, phone cables, electric power transmission lines, and railways [1-3]. Star-connected and neutrals grounded transformers which are connected by transmission lines are the most affected by such as induced current. Under the GIC conditions the transformers create unusual even and odd harmonics . These harmonics are able to triggering the relays improperly, overheating the generators and transformers windings and cores, which cause unstable. Operation of the power system and might result in the long term damage of the system components. When the GIC flows through the transformer windings, the DC magnetic flux is superimposed on the AC flux, so that the asymmetrical saturation occurs in magnetic cores of the transformers (half-cycle saturation), and their consumption of reactive power critically increases. Higher order harmonics will be generated which leads to tripping static var compensator (SVC) and shunt capacitors, and eventually may result in voltage collapse. Moreover, the contributed harmonics through the system affect the magnetization impedance and the relative permittivity of the magnetic core of the transformers significantly reduces. Furthermore, due to the effects of eddy currents that are related to the appearance of even harmonics and with increasing stray flux heat increases in the tank and fittings [4-11]. Fig. 1 illustrates the flow of the GIC which enter through neutrals grounded of the transformers to the transmission line. To estimate the geomagnetic disturbance impact on power systems needs to simulate the GIC flowing in the power network. In this paper, the GIC impacts on the grid-integrated hybrid PV-wind system transformers will be analyzed by using PSCAD/EMTDC software. Network topology, resistances, and orientation have a significant impact on the generated GIC by the geoelectric field [12].

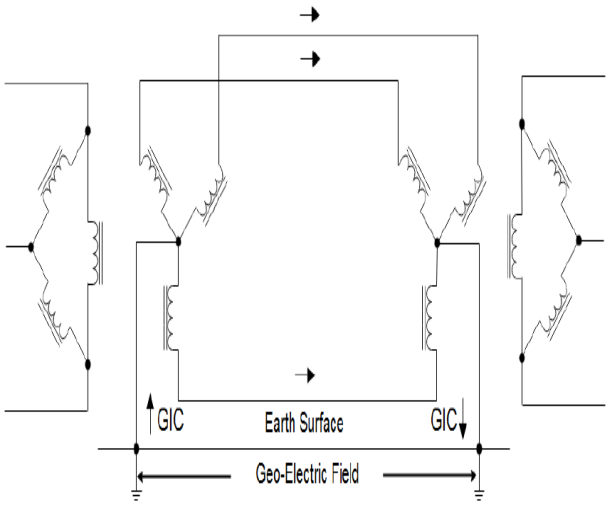

Fig. 1 The flow of GIC along the transmission line between two transformers

Manuscript published on November 30, 2019.
* Correspondence Author
Z M Khurshid*, College of Engineering, Universiti Tenaga Nasional, Jalan IKRAM-UNITEN, 43000 Kajang, Selangor, Malaysia.
N F Ab Aziz, College of Engineering, Universiti Tenaga Nasional, Jalan IKRAM-UNITEN, 43000 Kajang, Selangor, Malaysia.
M Z A Ab Kadir, College of Engineering, Universiti Tenaga Nasional, Jalan IKRAM-UNITEN, 43000 Kajang, Selangor, Malaysia.
Z A Rhazali, College of Engineering, Universiti Tenaga Nasional, Jalan IKRAM-UNITEN, 43000 Kajang, Selangor, Malaysia.

Retrieval Number: D5148118419/2019©BEIESP
DOI:10.35940/ijrte.D5148.118419
Journal Website: www.ijrte.org

Published By:
Blue Eyes Intelligence Engineering
& Sciences Publication

II. SYSTEM MODELING IN PSCAD

In this paper the hybrid system is carried out by using PSCAD program; it comprises of 2.1 MW wind farm, power storage, 2 MW PV farm, and load. The complete system is linked to the 33 kV grid through step-up transformer; the operation frequency of the system is set at 60 Hz. In addition, Pi-section is used between various parts of the hybrid system to represent the distance between them.

PV Farm Modeling Design

The PV farm consists of five units where each of them produces 400 kW. The generated DC power of each unit is converted to AC power by using a three-phase inverter that can be fed to the grid or to operate nearby load. The inverter is made up of the DC link capacitor, six insulated-gate bipolar transistors (IGBT) switches, LCL filter, and inverter control system. The current control technique is used to design a grid-connected inverter control system. The required parameters of a single unit PV system are presented in Table. 1 [13-16].

Table. 1 Specifications of PV cell and inverters

Specifications of One Unit PV Module	
Series connected modules per array	22
Parallel connected modules per array	215
Series connected cells per module	60
Parallel connected cells per module	1
Temperature	25 °C
Solar irradiation	1000 W/m^2
Inverters Specifications	
Switching frequency	3.6 kHz
Output voltage of inverter (line to line)	480 V
DC link capacitor	7800 µF
DC link voltage	780 V
LCL Filter Specifications	
Resistance of the filter (R)	2.6 Ω
Capacitance of the filter (C1)	100 µF
Capacitance of the filter (C2)	200 µF
Inductance of the filter (L1)	1.25 mH
Inductance of the filter (L2)	1.25 mH
Inductance of the filter (L3)	6.25 mH

Power Storage System Modeling Design

Various renewable energy (RE) system applications need energy storage in order to supply electrical energy during poor weather conditions or dark hours, especially in stand-alone ones of PV and WT systems. The most widely used storage devices are lead-acid batteries, usually, they are connected in the form of the battery bank and integrated to the system with an appropriate storage capacity to match the load demand when the RE sources cannot deliver enough electrical power [17]. In this work, the power storage system is implemented with the same program mentioned above and it includes a battery, a DC-DC converter, and a DC–AC inverter as illustrated in Fig. 2. During charging the battery, the converter works as a buck and as a boost during the discharging process [16]. The same inverter modeling design of PV system is used to feed the battery system from the AC bus during the charging process and vice versa during discharging the battery.

Wind Farm Modeling Design

The wind farm with a capacity of 2.1 MW is implemented by using WT (type I) with a fixed-speed generator. The generator is usually used to convert the produced mechanical power to electrical power. In this work, a 690V squirrel cage induction generator is employed with a constant speed of the rotor and integrated directly to a grid through the step-down transformer and 0.480 kV bus. The related models of wind energy, including mechanical and electrical parts are provided by PSCAD library. The specifications of WT and transformers are presented in Table. 2. The output power of the WT system is calculated based on equation 1[13, 14, and 18].

Table. 2 Specifications of WT and transformers

Specifications of WT and Induction Generator	
Wind speed (υ)	12 m/s
Air density (ρ)	1.23 kg/m^3
Power coefficient (Cp)	0.4 m
Rotor blade radius (r)	40 m
Rotor area	5026 m^2
Mechanical speed	314 [rad/s]
Efficiency of gearbox	0.97 pu
Wound rotor resistance of generator	0.00607 pu
Rated power	2.1 [MVA]
Specifications of Transformers	
Connection method	Δ / Y, Y / Δ
Voltage (line rms)	0.69/0.48 [kV], 0.48/33 [kV]
Rated power	100.0 [MVA], 100.0 [MVA]
Leakage reactance	0.15 [p.u], 0.15 [p.u]
Copper losses	0.01 [p.u], 0.0
No-load losses	Neglected

$$P = \frac{1}{2}\rho A v^3 C_p \qquad (1)$$

$$P = \frac{1}{2} \times 1.23 \times 5026 \times 12^3 \times 0.4 = 2.13\ MW$$

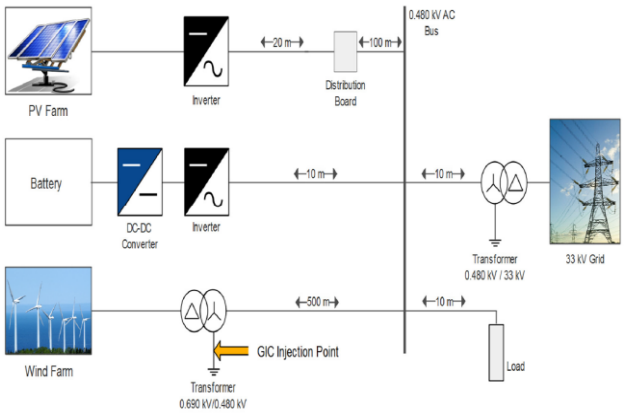

Fig. 2 Hybrid PV-wind system

GIC Source Modeling Design

In this work, the GIC is achieved by simple feedback DC source and connected to the neutral-to-ground point of WT transformer, the required GIC current is set at 100 A. As can be seen from Fig. 3, a root mean square (RMS) component and PI controller are used to filter out the harmonics from the measured dc component in the neutral connections.

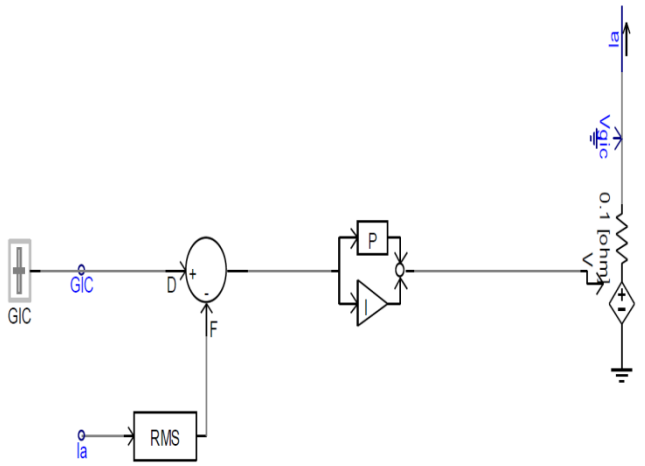

Fig. 3 GIC source in PSCAD/EMTDC

III. RESULTS AND DISCUSSION

Results without GIC

In this simulation case, the results are observed of the hybrid system under steady-state condition without injection of GIC to ensure the operation of the system under normal condition. As it is illustrated in Figs. 4-6, the output voltage and current waveforms are sinusoidal variations symmetrical around zero and clean which do not have harmonic distortion. In addition, the PV and WT systems are operated within specified real and reactive power limits.

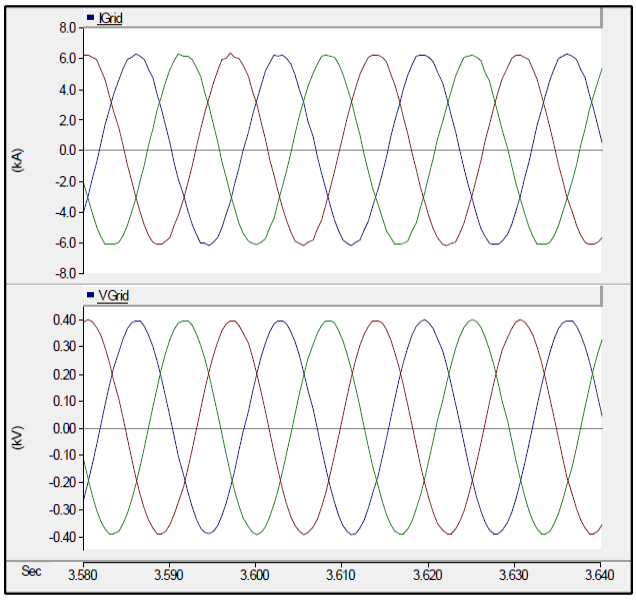

Fig. 4 Current and voltage output of hybrid system without GIC

The induction generator in a fixed speed WTs and transformers consume the reactive power; thus, the reactive power compensator such a capacitor bank needs to be linked to the system that includes such a type of inductive loads to correct the power factor. In this work, the capacitive load is linked to the system to compensate the reactive power, as illustrated in Fig. 5, the output power of the system is almost close to 4.1 MW and reactive power is close to zero, means that the system is operated at optimum efficiency.

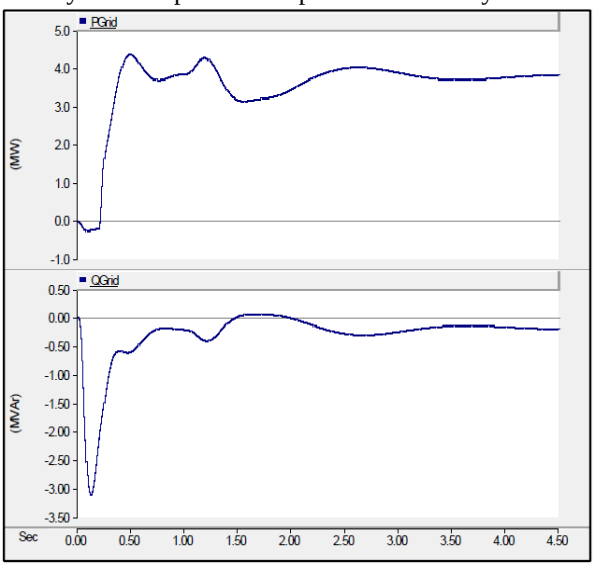

Fig. 5 Active and reactive power output of Hybrid system without GIC

In terms of transformer flux-current characteristic, in a steady-state condition, the flux in the transformer is in the linear region and the magnetizing current is sinusoidal. In this case, the accepted value and symmetrical around zero is observed as can be seen from Fig. 6.

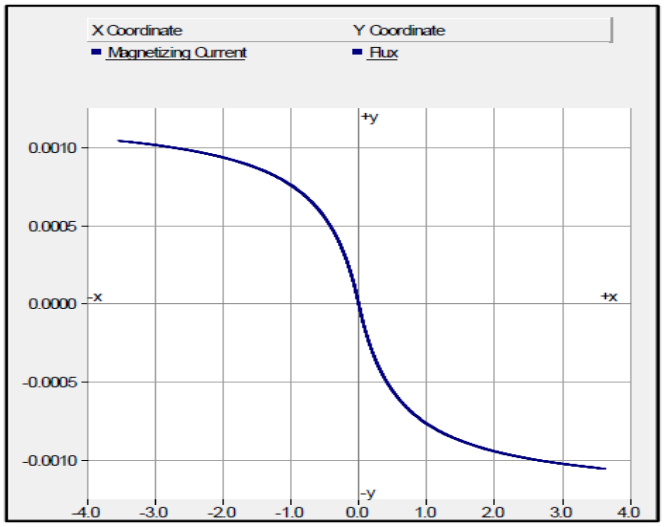

Fig. 6 Magnetization curve of WT transformer at normal operation without GIC

Results of GIC Effects without Mitigation Device

When a transformer is exposed to DC or low-frequency currents such as GIC during normal operation condition, DC flux is impressed in the transformer core and half-cycle saturation takes place. T

he magnetizing current is neither symmetrical nor sinusoidal with a DC offset and has relatively large peaks of current on the negative or positive side of the cycle not sinusoidal in both sides. As can be noticed from Fig. 7, when GIC is injected to the hybrid system through neutral of the WT transformer, the secondary AC current in the WT transformer which is connected to the 480 V bus is affected by GIC. The
magnetizing current is increased to 153 kA compared to 7.0 kA peak under normal conditions without GIC as presented in Fig. 7.

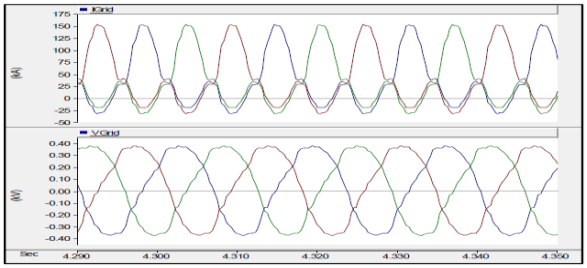

Fig. 7 Current and voltage output of Hybrid system with GIC

In addition, the reactive power of the hybrid system is increased to about 36.61 MVAR as it is shown in Fig. 8 from 0.200 MVAR in Fig. 5. This is because when the GIC is injected into the transformer, it will demand reactive power from the system and place a strain on the AC voltage.

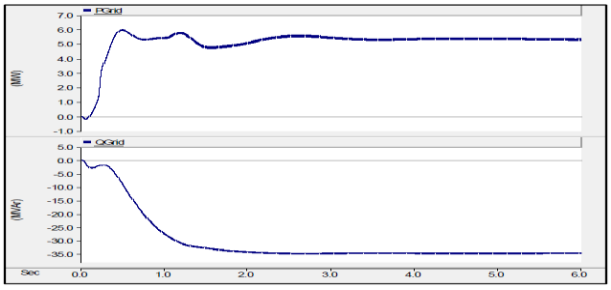

Fig. 8 Active and reactive power output of Hybrid system with GIC

Based on Fig. 9, the flux variation and its steady drift also become more and more positive, and the transformer enters to positive saturation region and half-cycle saturation when the system is affected by GIC.

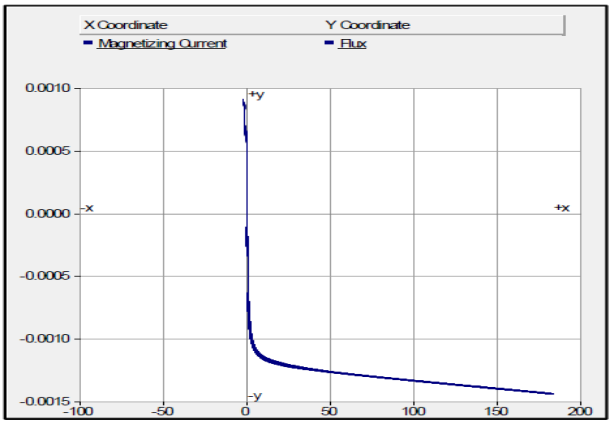

Fig. 9 Magnetization curve of WT transformer with GIC

Results of GIC Effects with Mitigation Devices

In this case, different GIC blocking devices have been applied and connected to the system in order to eliminate or mitigate the GIC effects in the hybrid system. Three types blocking devices such as 2.5 Ω and 5 Ω resistors [19], and also 5 μF capacitor are connected in the neutral-to-ground connection point of WT transformer where GIC injection path in different simulation cases respectively as illustrated in Fig. 10.

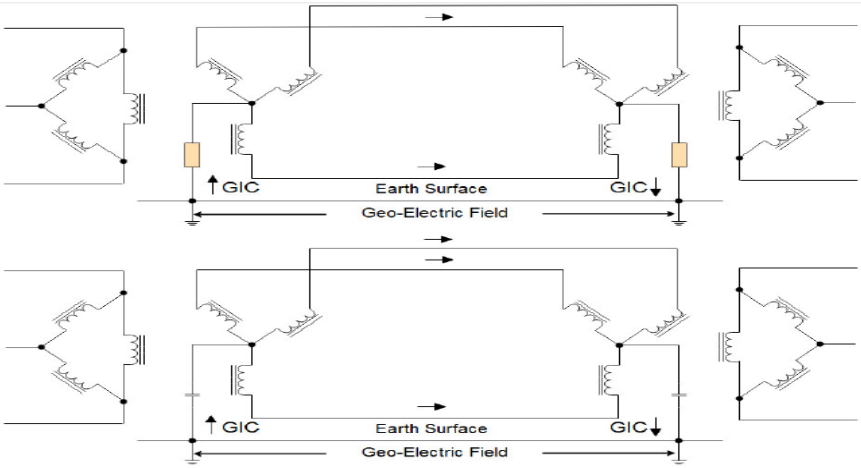

Fig. 10 Schematic of a GIC blocking devices in a transformer neutral

As can be seen from the obtained results in Figs. 11a and 12a, the GIC effects are reduced when 2.5 Ω blocking resistor is connected between the neutral-to-ground connection point of the WT transformer, however, some effects still exist as can be noticed from waveforms and transformer still consumes reactive power. For 5 Ω blocking resistor connection, the GIC effects are reduced more and better results are obtained as presented in Figs. 11b and 12b. The best results are obtained in this case when the capacitor blocking device is connected in the GIC path Figs. 11c and 12c; this is because the capacitor blocks all DC currents.

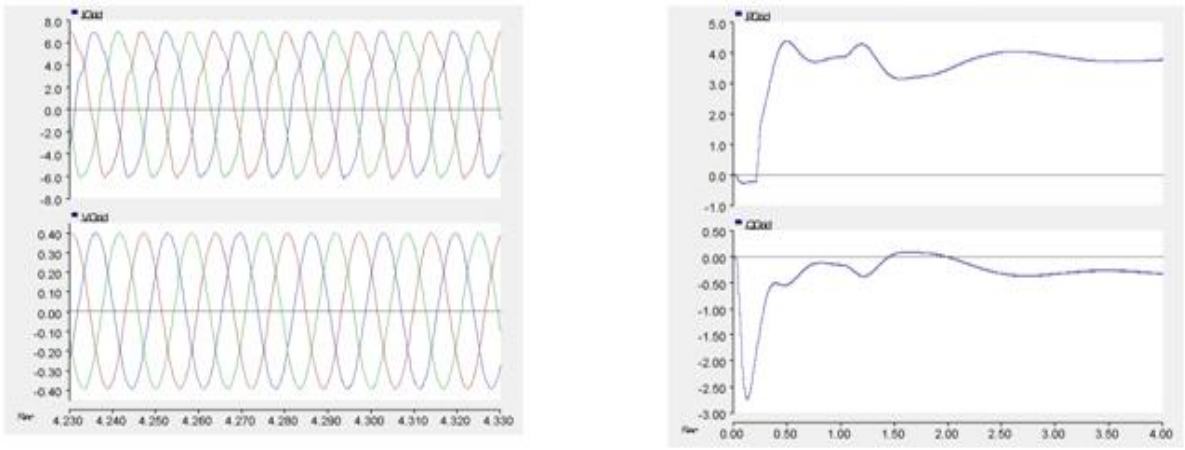

(a)

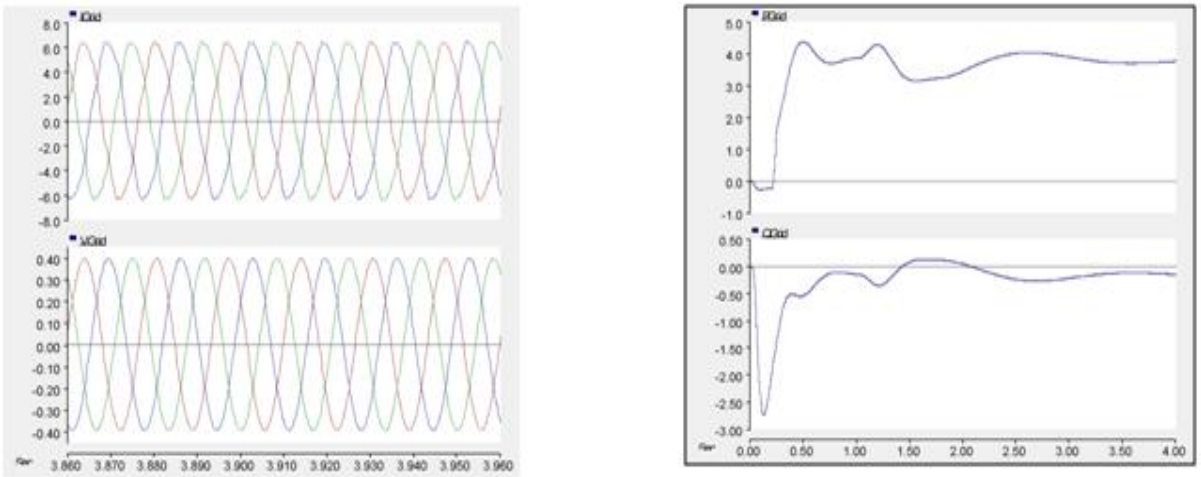

(b)

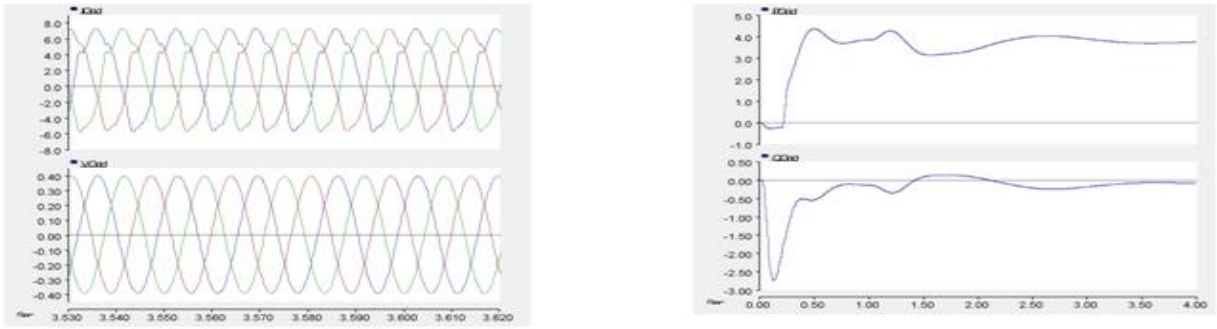

(c)

Fig. 11 Current, voltage and power outputs of Hybrid system with GIC when (a): 2.5 Ω; (b): 5 Ω; and (c): 5 µF capacitor blocking devices are applied

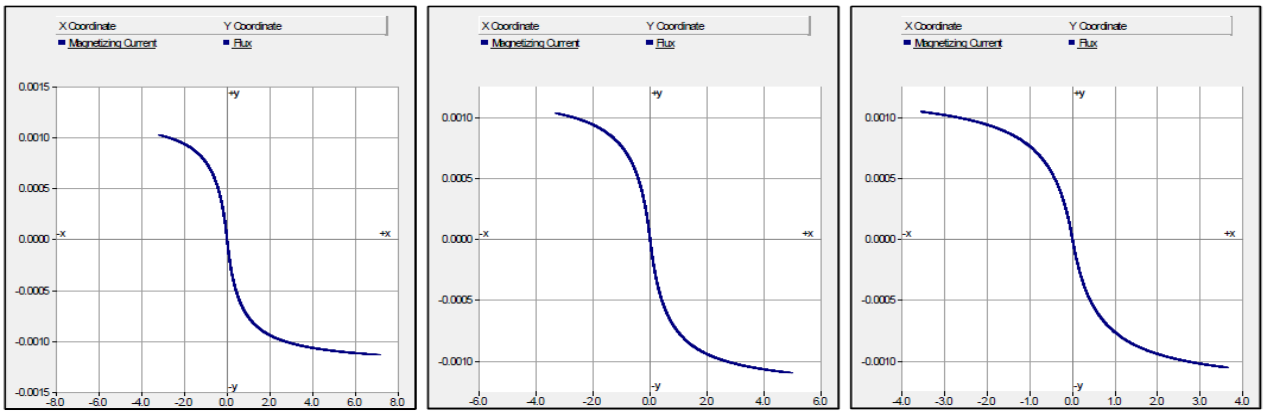

(a) **(b)** **(c)**

Fig. 12 Magnetization curve of WT transformer with GIC when (a): 2.5 Ω; (b): 5 Ω; and (c): 5 µF capacitor blocking devices are applied

IV. CONCLUSIONS

In this work, the effects of GIC on hybrid PV-wind system transformers were analyzed by using the PSCAD/EMTDC platform. The results have been obtained for different GIC effects analysis. At normal operation of the hybrid system without GIC, the current and voltage waveforms of the system output were clean and symmetrical around zero (linear operation). In addition, symmetrical flux and magnetizing current of the magnetic cores in the WT transformer are also observed. It is found that, when GIC is injected into the system through the neutral point of WT transformer, the magnetic cores in the WT transformer are saturated asymmetrically (Half-cycle saturation). Consequently, the magnitude of the output current of hybrid system has increased in the positive region which hence leads to the in increasing reactive power drastically. After the GIC blocking devices have been connected between the neutral-to-ground connection points of the WT transformer, the GIC effects have been mitigated. The best result in terms of mitigation has been obtained when 5 µF capacitor blocking device is connected between neutral-to-ground.

ACKNOWLEDGMENTS

The authors would like to thank the Ministry of Higher Education (MOHE) of Malaysia through a research grant of 20180112FRGS for the financial support to this research, also we would like to thank the College of Electrical and Electronic Engineering, Universiti Tenaga Nasional for their valuable facilities and support which lead to the successful achievement of this work. Special thanks to those who contributed to this project directly or indirectly.

REFERENCES

1. A.A. Hussein, M.H. Ali, Suppression of geomagnetic induced current using controlled ground resistance of transformer, Electric Power Systems Research, 140 (2016) 9-19.
2. S.P. Blake, P.T. Gallagher, J. McCauley, A.G. Jones, C. Hogg, J. Campanyà, C.D. Beggan, A.W. Thomson, G.S. Kelly, D. Bell, Geomagnetically induced currents in the Irish power network during geomagnetic storms, Space Weather, 14 (2016) 1136-1154.
3. C. Liu, Y. Li, R. Pirjola, Observations and modeling of GIC in the Chinese large-scale high-voltage power networks, Journal of Space Weather and Space Climate, 4 (2014) A03.
4. D. Boteler, R. Pirjola, Modeling geomagnetically induced currents, Space Weather, 15 (2017) 258-276.
5. Z. Zhao, F. Liu, Z. Cheng, W. Yan, L. Liu, J. Zhang, Y. Fan, Measurements and Calculation of Core-Based BH Curve and Magnetizing Current in DC-Biased Transformers, IEEE Transactions on Applied Superconductivity, 20 (2010) 1131-1134.
6. D. Boteler, "Methodology for simulation of geomagnetically induced currents in power systems," Journal of Space Weather and Space Climate, vol. 4, p. A21, (2014).
7. R. L. Bailey et al., "Modelling geomagnetically induced currents in midlatitude Central Europe using a thin-sheet approach," in Annales Geophysicae, 2017, vol. 35, no. 3: European Geosciences Union, pp. 751-761.
8. C. Haro, R.M. CASTRO, J. Ramirez-Niño, J.H.R. RODRIGUEZ, Core saturation effects of geomagnetic induced currents in power transformers, (2016).
9. D. M. Oliveira and C. M. Ngwira, "Geomagnetically induced currents: principles," Brazilian Journal of Physics, vol. 47, no. 5, pp. 552-560, (2017).
10. T. Zheng, G. Lu, P. Chen, T. Huang, and S. Chen, "Effects of geomagnetically induced currents on the transfer characteristics of current transformers," International Transactions on Electrical Energy Systems, vol. 27, no. 2, p. e2247, (2017).
11. T. Halbedl, H. Renner, and G. Achleitner, "Geomagnetically induced currents modelling and monitoring transformer neutral currents in Austria," e & i Elektrotechnik und Informationstechnik, vol. 135, no. 8, pp. 602-608, (2018).
12. R. Caraballo, Geomagnetically induced currents in Uruguay: Sensitivity to modelling parameters, Advances in Space Research, 58 (2016) 2067-2075.
13. Z. Mohammed, H. Hizam, C. Gomes, Lightning Strike Impacts on Hybrid Photovoltaic-Wind System, Indonesian Journal of Electrical Engineering and Computer Science, 8 (2017).
14. Z. Mohammed, H. Hizam, C. Gomes, Analysis of Lightning Transient Effects on Hybrid Renewable Energy Sources, in: International Conference on Lightning Protection (ICLP), IEEE, Poland, (2018).
15. R.-Y. Kim, S.-Y. Choi, I.-Y. Suh, Instantaneous control of average power for grid tie inverter using single phase DQ rotating frame with all pass filter, in: 30th Annual Conference of IEEE Industrial Electronics Society ECON, IEEE, Busan, South Korea, (2004), pp. 274-279.
16. A. Abdalrahman, A. Zekry, A. Alshazly, Simulation and implementation of grid-connected inverters, International Journal of Computer Applications, 60 (2012).
17. G. Bayrak, M. Lebeli, A PV based automation system for fish farms: An application study, in: 7th International Conference on Electrical and Electronics Engineering (ELECO), IEEE, (2011), pp. I-23-I-27.
18. B.C. Babu, K. Mohanty, Doubly-fed induction generator for variable speed wind energy conversion systems-modeling & simulation, International Journal of Computer and Electrical Engineering, 2 (2010) 141.

19. J. Kappenman, "Low-frequency protection concepts for the electric power grid: geomagnetically induced current (GIC) and E3 HEMP mitigation," FERC, Metatech Corporation, (2010).
20. Manikanthan, S.V., Padmapriya, T., "An efficient cluster head selection and routing in mobile WSN" International Journal of Interactive Mobile Technologies, 2019.